

Deuterodehalogenation Under Net Reductive or Redox-Neutral Conditions Enabled by Paired Electrolysis

Devin Wood¹ and Song Lin^{1*}

¹Department of Chemistry and Chemical Biology, Cornell University, Ithaca, NY 14853, USA.

*Corresponding authors: Song Lin (songlin@cornell.edu)

Abstract

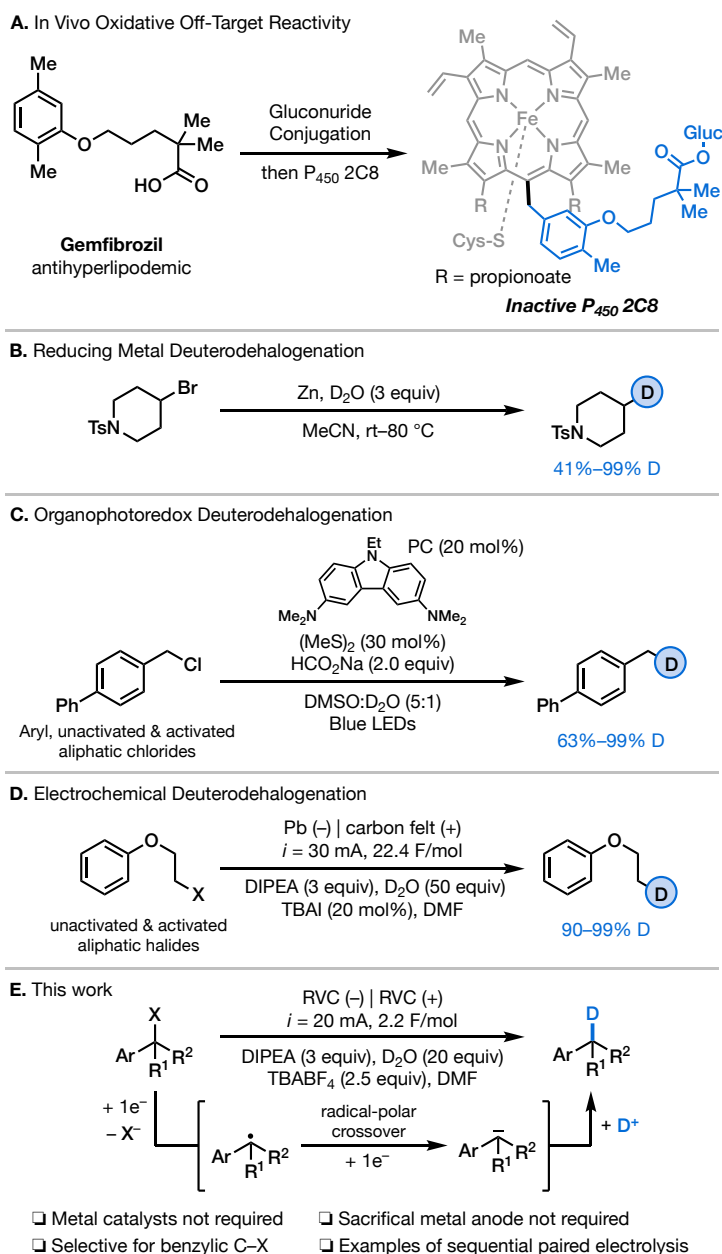
Interest in deuterated *de novo* active pharmaceutical ingredients (APIs) is increasing due to the release of the first FDA approved deuterated drug, deutetrabenazine. Deuteration also holds promise for kinetic isotope effect (KIE) regulated fine-tuning of active pharmaceutical ingredient performance. As such, methods for highly selective deuteration of organic molecules—particularly at positions that are prone to undergoing biochemical reactions—are highly desirable. Herein, we present an electrochemical method for the selective deuterodehalogenation of benzylic halides via a radical-polar crossover mechanism, using inexpensive deuterium oxide (D₂O) as the deuterium source. We demonstrate broad functional group compatibility across a range of aryl and heteroaryl benzylic halides. Furthermore, we uncover a sequential paired electrolysis regime, which permits switching between net reductive and overall redox-neutral reactions of sulfur-containing substrates simply by changing the identity of the sacrificial reductant employed.

Main Text

Extensive research has been devoted to understanding how active pharmaceutical ingredients (APIs) behave *in vivo*^[1] and how to prevent oxidative degradation, which is a major pathway in drug metabolism.^[2] Recent reports suggest that efficacy^[3] and toxicity metrics^[4] for certain APIs can be improved by deuteration of metabolically oxidizable^[5] C–H bonds.^[6] Ideally, kinetic isotope effects (KIEs) could be leveraged without compromising the conformational structure or reactivity of an API, thus allowing efficacy to be tuned after initial discovery to improve the pharmacokinetic profile. Such a strategy was recently employed with tetrabenazine^[7] by deuterating key methoxy groups that were identified as major sites for *in vivo* metabolism via oxidative degradation.^[8] Furthermore, deuteration can be employed to decrease the rate at which APIs react with off-target enzymes. For example, a major metabolite of the drug gemfibrozil reacts irreversibly with heme in P450 2C8 (Scheme 1A),^[9] although the rate of this inactivation was found to decrease when the metabolite was deuterated at the benzylic positions.^[9a]

Deuterodehalogenation stands out as a regiospecific route to construct C–D bonds from readily accessible C–X bonds, especially in a scaffold rich in C–H bonds where site-selective deuteration can be challenging with direct H/D exchange.^[10] We recently reported an electroreductive radical-polar crossover route for the formation of C(sp³)–C(sp³) bonds from disparately substituted alkyl halides,^{[11][12]} and we were interested in extending this approach to the deuteration of benzylic C–X bonds. While much of the literature is devoted to C(sp²)–X deuterodehalogenation,^[13–15] relatively few methods exist for the selective deuteration of C(sp³)–X bonds. Current strategies for sp³ deuterodehalogenation typically employ reducing metals such as magnesium^[16] and zinc^[17] (Scheme 1B) or expensive deuteride sources such as lithium aluminum deuteride.^[18] Modern routes include photoredox^[19] (Scheme 1C) and electrochemical^[20] activation (Scheme 1D) or employ radical chain processes.^[21] While these methods provide mild alternatives to reducing metal-mediated processes, they rely on high loadings of photocatalysts or toxic lead-based electrodes that may pose challenges in practical applications. In addition, many of these methods are not selective for one type of aliphatic halide, showing reactivity towards both activated and unactivated halides, and in some cases, also aryl halides.

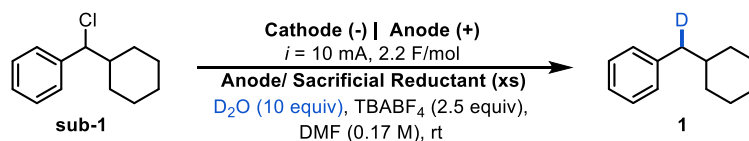
Considering these challenges, we sought to harness a radical-polar crossover approach towards the facile deuteration of benzylic sites of complex molecules that might be of medicinal relevance (Scheme 1E). Here, we show it is possible to achieve efficient and selective activation of benzyl halides by leveraging the relatively low potentials for the reduction of benzylic C–X bonds and the resultant benzyl radicals, thus



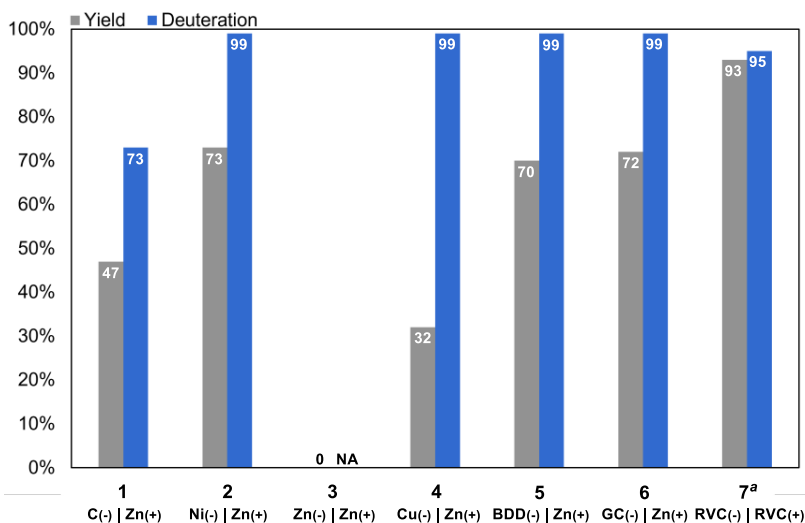
Scheme 1. (A) Example of an API where off-target oxidation leads to inactivation of a cytochrome enzyme and causes drug-drug interactions. (B)–(D) Examples of current methods for aliphatic deuterodehalogenation. (E) Electrochemically driven deuterodehalogenation of benzylic halides developed in this work.

accomplishing an overall two-electron reduction to form benzyl anions, which can then be deuterated using D_2O as a D^+ source.^[11] Additionally, we demonstrate that a paired-electrolysis manifold using a homogenous sacrificial reductant instead a sacrificial metal anode can mediate highly selective deuteration in the presence of other redox-sensitive chemotypes, such as complex heterocycles, acidic functional groups (e.g., alcohols and amides), and esters. Importantly, this method is highly selective for the functionalization of benzylic chlorides over unactivated alkyl and aryl halides.

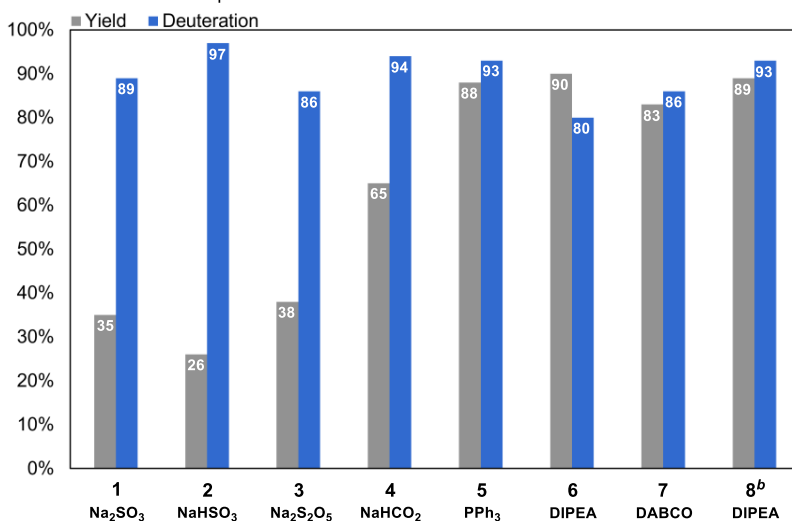
Our initial discovery effort focused on the electroreductive deuteration of benzylic chloride **sub-1** under conditions analogous to our previously reported cross-electrophile-coupling reaction—which is selective for alkyl halides bearing an anion stabilizing group^[11]—but using D_2O as an electrophile (Scheme 2). Here, a key challenge that needed to be addressed was the cathodic hydrogen evolution reaction (HER), which could diminish Faradaic efficiency as well as lead to unwanted consumption of the deuterium source. Electrode materials with high HER overpotentials^[22] were thus considered. We initially found that a graphite cathode and zinc anode (C(-) | Zn(+), Scheme 2A, entry 1) facilitated the formation of deuterodehalogenation product **1**, albeit with moderate levels of deuterium incorporation when D_2O (5



A. electrode optimization



B. sacrificial reductant optimization



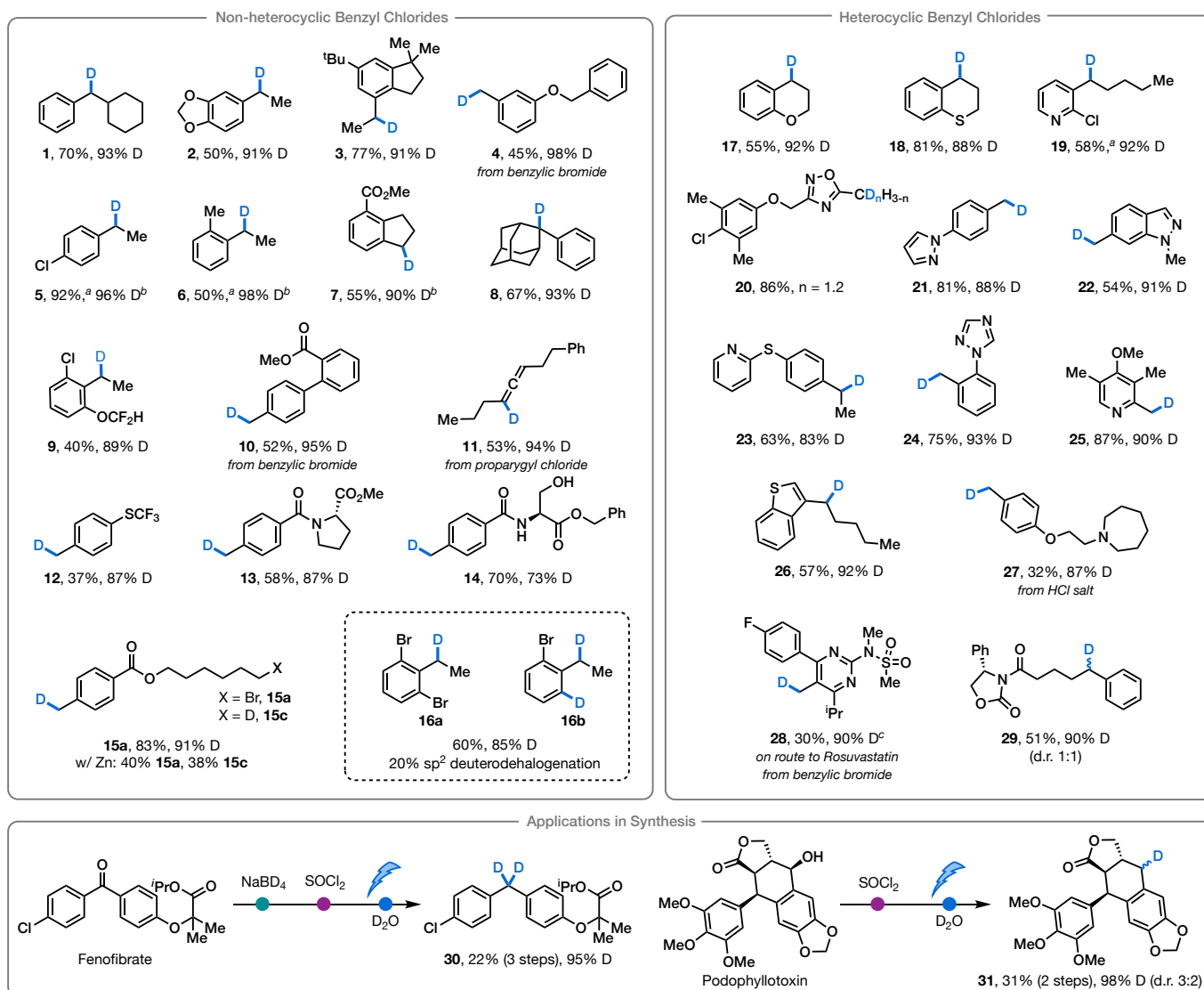
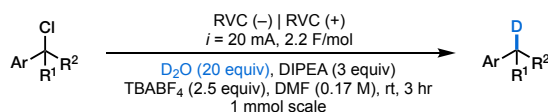
Scheme 2. (A) Optimization of cathode and anode. Conditions: benzylic chloride (**sub-1**; 0.5 mmol), tetrabutylammonium perchlorate ($TBAClO_4$; 3 equiv), DMF:DME (2:1, 0.17 M), D_2O (5 equiv), constant current $i = 5$ mA, charge 2.2 F/mol. Yield and deuterium incorporation were determined by analysis of 1H NMR spectra (see Section 8 of the Supporting Information for details). (B) Optimization of sacrificial reductants. Conditions: **sub-1** (0.5 mmol), sacrificial reductant (3 equiv), tetrabutylammonium tetrafluoroborate ($TBABF_4$; 2.5 equiv), DMF (0.17 M), D_2O (10.0 equiv), constant current $i = 20$ mA, charge 2.2 F/mol. Yield and deuterium incorporation were determined by analysis of 1H NMR spectra (see Section 8 of the Supporting Information). Abbreviations: BDD = boron-doped diamond, GC = glassy carbon, RVC = reticulated vitreous carbon. Footnotes: ^awith PPh_3 (3 equiv) as sacrificial reductant. ^bwith D_2O (20 equiv).

equiv) was employed as the deuterium source. Improvements in yield and deuterium incorporation were observed with nickel (Ni), boron-doped diamond (BDD), and glassy carbon (GC) cathodes (entries 2, 5, & 6). The particular improvements achieved with BDD and GC are attributed to their high HER overpotentials (See Table S1 for data and references).

In the course of reaction optimization, we routinely observed passivation of the cathode by zinc(II) salts that were generated by the anodic process and would plate out as an inhomogeneous layer. This passivation typically led to gradually decreased reaction efficiency as electrolysis proceeded. Seeking to prevent this passivation, we alternatively explored a paired electrolysis system. We employed reticulated vitreous carbon (RVC)—which exhibits HER overpotentials similar to GC^[23] but is less expensive and disposable—as both the cathode and anode. Additionally, since RVC has a higher surface area than GC, a greater current could be applied, leading to faster reaction times. Using this paired electrolysis system and employing triphenylphosphine (PPh₃) as the sacrificial electron donor, we observed quantitative conversion of benzyl chloride **sub-1** to the desired product **1** with excellent deuterium incorporation (entry 7; 92% yield, 95% D).

With optimal cathodic conditions in hand, we next sought to optimize the sacrificial reductant. A facile anodic process was desirable to ensure broad functional group tolerance (e.g., oxidizable heterocycles, alcohols, or electron rich arenes). We also sought to avoid sacrificial reductants that would generate protons upon oxidation and thereby possibly contribute to competing protonation reactions. We screened a series of alternative sacrificial reductants^[24] and the results are summarized in Scheme 2B. We found sulfite salts to be poorly soluble (entries 1-3) in the *N,N*-dimethylformamide (DMF) solvent used, leading to lower product yields than achieved with PPh₃. On the other hand, excellent yields and high deuterium incorporation were achieved when using *N,N*-diisopropylethylamine (DIPEA) or 1,4-diazabicyclo[2.2.2]octane (DABCO) (entries 6 and 7), although 20 equivalents of D₂O were used in the optimal condition to ensure H⁺ formed in the anodic counter reaction did not significantly impact deuterium incorporation (entry 8). Ultimately, DIPEA was selected as the ideal sacrificial reductant due to its low cost, good atom economy when compared to PPh₃, and lower oxidation potential ($E_{p/2} = 0.73$ and 1.05 V vs. SCE for DIPEA and PPh₃, respectively), which would ensure good functional group compatibility.

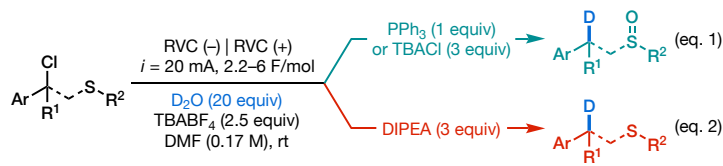
We next assessed the scope of the deuterodehalogenation reaction and found a wide range of organic functionalities were tolerated (Scheme 3). Electron rich aryl and heteroaryl functionalities were found to be suitable substrates, yielding products **2**, **12**, **17**, **18**, and **21–24**. Acidic protons were also tolerated, albeit at the expense of a slight decreases in deuterium incorporation (products **14**, **20**, **28**, **29**, and **31**). Furthermore, our method was able to discern between benzylic chlorides in the presence of aryl halides and aliphatic bromides (**5**, **9**, **15**, **19**, and **20**), and only in the case of 1,3-dibromo-2-(1-chloroethyl)benzene (**sub-16**) did we observe partial debromodeuteration of the aryl group with a 3:1 selectivity for the desired benzylic deuteration product (**16a**). Density functional theory calculations carried



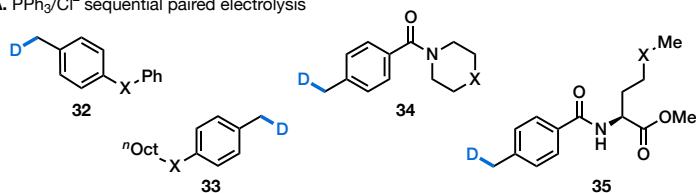
Scheme 3. Reaction scope. Conditions: Benzylic chloride (1 mmol, 1 equiv), D_2O (20 equiv), *N,N*-diisopropylethylamine (3 equiv), TBABF_4 (2.5 equiv), DMF (0.17 M), RVC anode, RVC cathode, undivided cell, constant current $i = 20$ mA, charge 2.2 F/mol. All yields are isolated and deuterium incorporation in products was determined by analysis of ^1H NMR and ^{13}C NMR spectra, unless otherwise noted. Footnotes: ^aYield determined by NMR using 1,3,5-trimethoxy benzene as internal standard. ^bDeuterium incorporation determined by mass spectrum analysis. ^cWith 3:1 $\text{D}_2\text{O}:\text{AcOD}$ (20 eq. D^+), constant current $i = 25$ mA, charge 4.0 F/mol.

out at the (U)B3LYP/6-31+G(d) level of theory indicate a thermodynamic preference for benzylic chloride reduction over aryl bromide reduction during the initial single electron transfer event ($E_{\text{red}}(\text{C}(\text{sp}^2)-\text{Br}) \sim -1.25$ V vs. SCE; $E_{\text{red}}(\text{C}(\text{sp}^3)-\text{Cl}) \sim -0.38$ V vs. SCE with DMF as solvent; see Section 5 of the Supporting Information for further details). Additionally, aliphatic bromide **sub-15** was tolerated with pristine selectivity for the benzylic chloride, reactivity not observed under chemical conditions utilizing stoichiometric zinc^[16] (see Section 8 of the Supporting Information for control experiment details). Finally, a range of heteroaryl containing benzylic halides were well tolerated yielding products **17–29**, suggesting the broader utility of this

approach for the facile synthesis of more complex compounds for medicinal chemistry applications. Of note, over-deuteration was observed for **20** owing to further deuterium incorporation at the acidic benzylic position via H⁺/D⁺ exchange.

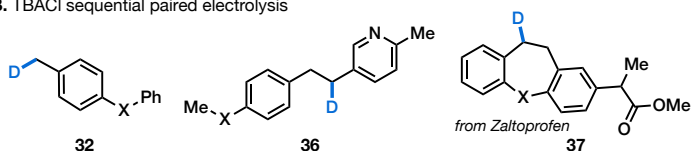


A. PPh₃/Cl⁻ sequential paired electrolysis



Substrate	Product	Reductant	X	Yield (%)	Deuterium (%)
sub-32	32	DIPEA ^a	S	68	93
sub-33	33	DIPEA ^a	S	72	80
sub-34	34	DIPEA ^a	S	53	88
sub-35	35	DIPEA ^a	S	68	80
sub-32	32-ox	PPh ₃ ^b	S=O	74	97
sub-33	33-ox	PPh ₃ ^b	S=O	53	97
sub-34	34-ox	PPh ₃ ^b	S=O	53	94
sub-35	35-ox	PPh ₃ ^b	S=O	52	96

B. TBACl sequential paired electrolysis



Substrate	Product	Reductant	X	Yield (%)	Deuterium (%)
sub-32	32	DIPEA ^a	S	68	93
sub-36	36	DIPEA ^a	S	44	88 ^d
sub-37	37	DIPEA ^a	S	88	>99
sub-32	32-ox	TBACl ^c	S=O	52	83
sub-36	36-ox	TBACl ^c	S=O	30	88
sub-37	37-ox	TBACl ^c	S=O	52	89



Scheme 4. Substrate scope for chlorine-mediated oxidation utilizing (A) substrate Cl⁻ or (B) TBACl as the chlorine source. Footnotes: ^aBenzylic chloride (1 mmol, 1 equiv), D₂O (20 equiv), DIPEA (3 equiv), TBABF₄ (2.5 equiv), DMF (0.17 M), RVC anode, RVC cathode, undivided cell, constant current *i* = 20 mA, charge 2.2 F/mol. ^bBenzylic chloride (1 mmol, 1 equiv), D₂O (20 equiv), PPh₃ (1.1 equiv), TBABF₄ (2.5 equiv), DMF (0.17 M), RVC anode, RVC cathode, undivided cell, constant current *i* = 20 mA, charge 5.0 F/mol. ^cBenzylic chloride (1 mmol, 1 equiv), D₂O (20 equiv), TBACl (3 equiv), TBABF₄ (1.5 equiv), DMF (0.17 M), RVC anode, RVC cathode, undivided cell, constant current *i* = 20 mA, charge 3.2 F/mol. ^dDeuterium incorporation determined by mass spectrum analysis.

position via H⁺/D⁺ exchange.

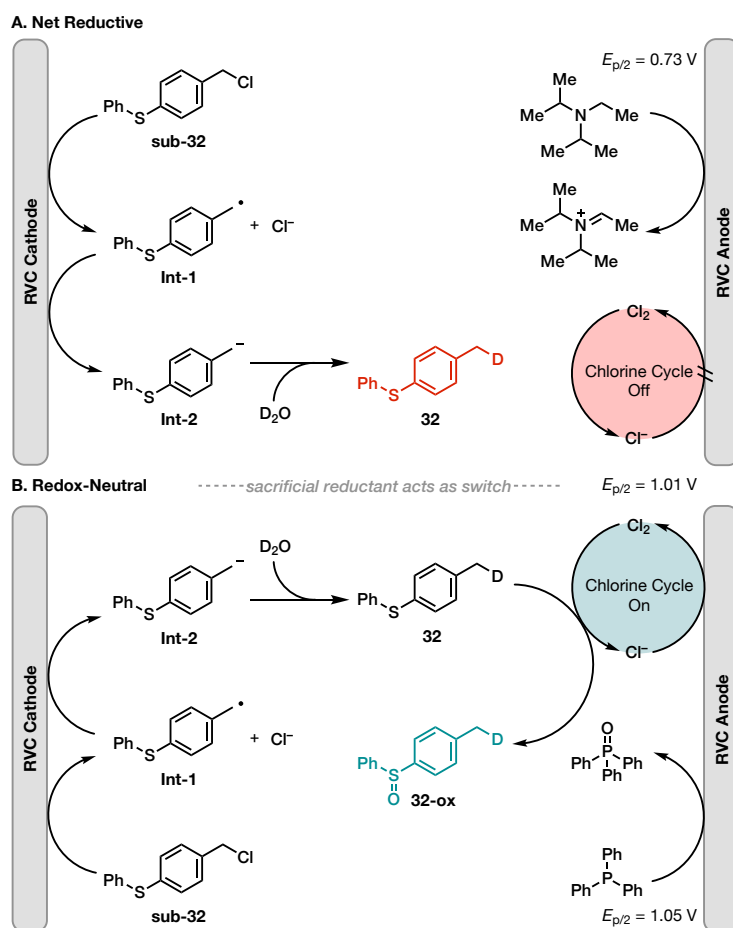
Interestingly, we found that when PPh₃ was employed as the sacrificial reductant instead of DIPEA for substrates containing a sulfide group, we could selectively induce sulfide oxidation to form the corresponding sulfoxide while also achieving the desired deuteration (Scheme 4, equation 1). In contrast, using DIPEA led to formation of the expected deuterodehalogenation product with no change in the sulfur oxidation state (equation 2).

We investigated the origin of this divergent chemoselectivity using cyclic voltammetry (CV). Experimental data for all oxidizable species were collected and the half-wave potentials (referenced to SCE) were found to be 0.73 V for DIPEA, 1.05 V for PPh₃, 1.01 V for tetrabutylammonium chloride (TBACl, used as a surrogate for Cl⁻ generated from substrate reduction), and 1.65 V for sulfide **sub-32** (Figure S1). On the basis of these data, direct anodic oxidation of the sulfide seems unlikely. We hypothesized that Cl₂ formed at the anode—derived from Cl⁻ via substrate reduction—could be mediating sulfide oxidation, reactivity that is known in the literature.^[25] Indeed, CV experiments conducted with TBACl in the presence of **sub-32** revealed current enhancement with increasing substrate concentration, supporting electrogenerated Cl₂ as the oxidant (Figure S2). Thus, we propose that in the reaction

using DIPEA as a sacrificial reductant, the potentials are not sufficiently oxidizing to generate Cl_2 , and hence only the deuterated product **32** is generated. In contrast, because PPh_3 and Cl^- have overlapping oxidation potentials, Cl_2 is generated simultaneously with oxidation of PPh_3 , favoring the production of **32-ox**. It is also possible that electrophilic ClPPh_3^+ was generated in this process,^[26] which could either react with D_2O to form triphenylphosphine oxide or with the sulfide substrate to eventually give rise to the sulfoxide. These distinct mechanistic pathways are illustrated in Scheme 5.

With this insight in hand, we identified two conditions suitable to perform both sulfur oxidation and deuterodehalogenation. In addition to conditions using PPh_3 (**32-ox**, **33-ox**, **34-ox**, **35-ox**; Scheme 4A), we also found that TBACl could be used as the sacrificial reductant instead, promoting the deuterodehalogenation-oxidation, generating **32-ox**, **36-ox**, and **37-ox** (Scheme 4B). Furthermore, C–H oxidation of **sub-38** with pendant thiophene^[27] was achieved under these conditions to give **38-ox** in good yield. These two methods are complementary in that the one using TBACl requires less total charge and shorter reaction time but that the system using PPh_3 shows better substrate generality due to lower concentration of anodically generated Cl_2 . In corresponding experiments employing DIPEA as the sole sacrificial reductant, there is no observation of sulfur oxidation (**32–38**). Thus, by changing the sacrificial electron donor, the sulfur oxidation cycle can be turned on or off. The ability to selectively run a reduction reaction while concomitantly oxidizing another functional group in the same molecule highlights the unique power of electrochemistry to effect multiple redox events in one reaction and take full advantage of the Faradaic efficiency of a cell via sequential paired electrolysis.^[28] This reactivity control is also of practical significance given the prevalence of sulfur-containing molecules in medicinal chemistry.^[29]

In conclusion, we have presented a mild electrochemical method for the selective deuterodehalogenation of benzylic chlorides using D_2O , without the need for a metal catalyst or a sacrificial



Scheme 5. Proposed mechanism for formation of **32** under reductive conditions and proposed mechanism for the formation of **32-ox** under redox neutral conditions with a chlorine mediated oxidation. The product formed depends on sacrificial reductant used.

anode. Our methodology affords access to deuterated analogs of highly functionalized molecules including those containing medically relevant motifs. Furthermore, we have shown that based on the choice of sacrificial reductant, it is possible to achieve multisite oxidation state changes in a single molecule during the electrochemical reaction. We anticipate that both electroreductive radical-polar crossover and sequential paired electrolysis will prove to be general and effective strategies in the future development of synthetically useful electrochemical transformations.

Acknowledgements:

We thank Dr. W. Zhang for experimental support and discussions, Dr. I. Keresztes for assistance in NMR data analysis, Dr. Y. Wang for computational assistance, and Dr. D. Lehnher for valuable discussions and suggestions.

Funding

Funding for this study was provided by the National Institute of General Medical Sciences (R01GM134088). S.L. thanks the Research Corporation for Science Advancement for a Cottrell Scholar Award. This study made use of the Cornell University NMR facility supported by the National Science Foundation (CHE-1531632).

Competing interests:

The authors declare no competing interests.

References and Notes:

1. Y. Li, Q. Meng, M. Yang, D. Liu, X. Hou, L. Tang, X. Wang, Y. Lyu, X. Chen, K. Liu, A-M. Yu, Z. Zuo, H. Bi, *Acta Pharmaceutica Sinica B*, **2019**, 9, 1113 – 1144.
1. 2. U. Zanger, M. Turpeinen, K. Klein, M. Schwab, *Anal. Bioanal. Chem.*, **2008**, 392, 1093 – 1108.
2. A. Kerekes, S. Esposito, R. Doll, J. Tagat, T. Yu, Y. Xiao, Y. Zhang, D. Prelusky, S. Tevar, K. Gray, G. Terracina, S. Lee, J. Jones, M. Liu, A. Basso, E. Smith, *J. Med. Chem.*, **2011**, 54, 201 – 210.
3. Z. Zhan, X. Peng, Y. Sun, J. Ai, W. Duan, *Chem. Res. Toxicol.* **2018**, 31, 1213–1218.
4. For examples of enzymes that oxidize C-H bonds see: (a) S. Cargnin, M. Serafini, T. Pirali, *Future Med. Chem.*, **2019**, 11, No. 16 (b) A. Khan, S. Misenko, A. Thandoni, D. Schiff, S. Jhavar, S. Bunting, B. Haffty, *Oncotarget*, **2018**, 9, 25833–25841.
5. For a review on deuterium in medicinal chemistry, see: T. Pirali, M. Serafini, S. Cargnin, A. Genazzani, *J. Med. Chem.*, **2019**, 62, 5276–5297.
6. T. Belete, *Drug Design, Development, and Therapy*, **2022**, 16, 3465-3472.
7. F. Schneider, M. Bradbury, T. Baillie, D. Stamler, E. Hellriegel, D. Cox, P. Loupe, J-M. Savola, L. Rabinovich-Guilatt, *Clinical and Trans. Science*, **2020**, 13, 707 – 717.
8. For studies on oxidative reactivity of Gemfibrozil, see: (a) B. Baer, R. DeLisle, A. Allen, *Chem. Res. Toxicol.*, **2009**, 22, 1298 – 1309. (b) S. Orr, S. Ripp, T. Ballard, J. Henderson, D. Scott, R. Obach, H. Sun, A. Kalgutkar, *J. Med. Chem.*, **2012**, 55 4896 – 4933. (c) M. Zhao, J. Zhi, W. Li, C. Guan, C. Sun, Y. Peng, J. Zheng, *Chem. Res. Toxicol.*, **2022**, 35, 1257 – 1266.

9. For reviews pertaining to hydrogen-isotope exchange reactions, which tend to accommodate multisite H/D exchange, see: (a) M. Valero, V. Derdau, *J. Label. Compd. Radiopharm.*, **2019**, 63, 266 – 280. (b) D. Hesk, *J. Label. Compd. Radiopharm.*, **2019**, 63, 247 – 265. (c) W. Lockley, J. Heys, *J. Label. Compd. Radiopharm.*, **2010**, 53, 635 – 644. (d) T. Junk, W. Catallo, *Chem. Soc. Rev.*, **1997**, 26, 401 – 406.
10. (a) W. Zhang, L. Lu, W. Zhang, Y. Wang, S. Ware, J. Mondragon, J. Rein, N. Strotman, D. Lehnerr, K. See, S. Lin, *Nature*, **2022**, 604, 292 – 297. (b) W. Zhang, S. Lin, *J. Am. Chem. Soc.* **2020**, 142, 20661–20670.
11. For examples of early work on electroreductive chemistry of alkyl halides that inspired our work, see: (a) J-Y. Nédélec, H. Ait-Haddou-Mouloud, J. C. Folest, J. Périchon, *J. Org. Chem.*, **1988**, 53, 4720 – 4724. (b) J. A. Cleary, M. S. Mubarak, K. L. Vieira, M. R. Anderson, D. G. Peters, *J. Electroanal. Chem. Interfacial Electrochem.* **1986**, 198, 107–124. (c) C. P. Andrieux, I. Gallardo, J. M. Saveant, *J. Am. Chem. Soc.* **1989**, 111, 1620–1626.
12. For electrochemical methods, see: (a) C. Liu, S. Han, M. Li, X. Chong, B. Zhang, *Angew. Chem. Int. Ed.* **2020**, 59, 18527 – 18531. (b) J. Cockrell, R. J. Murray, *Electrochem. Soc.*, **1972**, 119, 849. (c) R. Renaud, *Can. J. Chem.*, **1974**, 52, 376–380. (d) J. Grimshaw, J. J. Trocha-Grimshaw, *Chem. Soc., Perkin Trans.*, **1975**, 2, 215–218. (e) L. Lu, H. Li, Y. Zheng, F. Bu, A. Lei, *CCS Chem.*, **2020**, 2, 2669–2675.
13. For chemical methods, see: (a) M. Kuriyama, N. Hamaguchi, G. Yano, K. Tsukuda, O. Onomura, *J. Org. Chem.* **2016**, 81, 19, 8934–8946. (b) M. Kuriyama, G. Yano, H. Kiba, T. Morimoto, K. Yamamoto, Y. Demizu, O. Onomura, *Org. Process Res. Dev.* **2019**, 23, 8, 1552–1557. (c) C. Donald, T. Moss, G. Noonan, B. Roberts, E. Durham, *Tet Lett.*, **2014**, 22, 3305 – 3307. (d) T. Hokamp, A. Dewanji, M. Lubbesmeyer, C. Muck-Lichtenfeld, E-U. Wurthwein, A. Studer, *Angew. Chem. Int. Ed.*, **2017**, 56, 13275 – 13278.
14. For a review on deuterium and tritium labeling, see: S. Kopf, F. Bourriquen, W. Li, H. Neumann, K. Junge, M. Beller, *Chem. Rev.* **2022**, 122, 6, 6634–6718.
15. (a) A. Egorov, A. Anisimov, *J. Organometallic Chem.*, **1994**, 479, 197 – 198. (b) A. Egorov, A. Anisimov, *J. Organometallic Chem.*, **1995**, 495, 131 – 134.
16. A. Xia, X. Xie, X. Hu, W. Xu, Y. Liu, *J. Org. Chem.*, **2019**, 84, 13841–13857.
17. (a) E. Eliel, *J. Am. Chem. Soc.*, **1949**, 71, 3970 (b) M. Mills, R. Sonstrom, Z. Vang, J. Neill, H. Scolati, C. West, B. Pate, J. Clark, *Angew. Chem. Int. Ed.*, **2022**, 61, e2022072.
18. (a) Y. Li, Y-M. Lin, Y. Liu, Y. Zhang, L. Gong, *Nature Comm.*, **2021**, 12, 2894. (b) Y. Gu, H. Yin, M. Wakeling, J. An, R. Martin, *ACS Catal.*, **2022**, 12, 1031–1036.
19. P. Li, C. Guo, S. Wang, D. Ma, T. Feng, Y. Wang, Y. Q, *Nature Comm.*, **2022**, 13, 3774.
20. (a) D. Spiegel, K. Wiberg, L. Schacherer, M. Medeiros, J. Wood, *J. Am. Chem. Soc.* **2005**, 127, 12513–12515. (b) V. Soulard, G. Villa, D. Vollmar, P. Renaud, *J. Am. Chem. Soc.*, **2018**, 140, 155–158.
21. For a compiled list of HER overpotentials vs. SCE, see: D. Heard, A. Lennox, *Angew. Chem. Int. Ed.*, **2020**, 59, 18866 – 18884.
22. A. Koca, *Int. J. Hydrogen Energy*, **2009**, 34, 2107–2112.
23. (a) M. Rathnayake, J. Weaver, *Org. Lett.*, **2019**, 21, 9681–9687. (b) L. Peng, Z. Li, G. Yin, *Org. Lett.*, **2018**, 20, 1880–1883. (c) A. Chmiel, O. Williams, C. Chernowsky, C. Yeung, Z. Wickens, *J. Am. Chem. Soc.*, **2021**, 143, 10882–10889. (d) K. Hayashi, J. Griffin, K. Harper, Y. Kawamata, P. S. Baran, *J. Am. Chem. Soc.*, **2022**, 144, 5762 – 5768.
24. (a) C. Bottecchia, D. Lehnerr, F. Lévesque, M. Reibarkh, Y. Ji, V. L. Rodrigues, H. Wang, Y.-h. Lam, T. P. Vickery, B. M. Armstrong, K. A. Mattern, K. Stone, M. K. Wismer, A. N. Singh, E. L. Regalado, K. M. Maloney, N. A. Strotman, *Org. Process Res. Dev.* **2022**, 26, 2423–2437. (b) J. Strehl, G. Hilt, *Eur. J. Org. Chem.*, **2022**, 1, 35–39. (c) K. Mitsudo, Y. Tachibana, E. Sato, S. Suga, *Org. Lett.* **2022**, 24, 46, 8547–8552. (d) K. Mitsudo, R. Matsuo, T. Yonezawa, H. Inoue, H. Mandai, S. Suga, *Angew. Chem. Int. Ed.*, **2020**, 59, 7803–7807.
25. R. Appel, *Angew. Chem. Int. Ed.*, **1975**, 14, 801 – 811.
26. H. Coonradt, H. Hartough, G. Johnson, *J. Am. Chem. Soc.*, **1948**, 70, 2564–2568.

27. For other examples of sequential paired electrolysis, see: (a) J. Strehl, M. Abraham, G. Hilt, *Angew. Chem. Int. Ed.*, **2021**, *60*, 9996–1000. (b) A. Lindsay, P. Kilmartin, J. Sperry, *J. Org. Biomol. Chem.*, **2021**, *19*, 7903–7913. (c) T. Kashiwagi, T. Fuchigami, T. Saito, S. Nishiyama, M. Atobe, *Chem. Lett.*, **2014**, *43*, 799–801.
28. Muhamad Mustafa & Jean-Yves Winum (2022) The importance of sulfur-containing motifs in drug design and discovery, *Expert Opinion on Drug Discovery*, *17*:5, 501-512, DOI: 10.1080/17460441.2022.2044783.